Molecular Crystals and Liquid Crystals
Publication details, including instructions for authors and subscription information:
http://www.tandfonline.com/loi/gmcl16

The Stable Inhomogeneities of Mixtures and the Permanent Liquid-Crystalline Diffraction Gratings

Antoni Adamczyk [a]
[a] Institute of Physics, Warsaw Technical University, Koszykowa 75, 00-662, Warsaw, Poland
Version of record first published: 28 Mar 2007.

To cite this article: Antoni Adamczyk (1977): The Stable Inhomogeneities of Mixtures and the Permanent Liquid-Crystalline Diffraction Gratings, Molecular Crystals and Liquid Crystals, 42:1, 81-96

To link to this article: http://dx.doi.org/10.1080/15421407708084498

Mol. Cryst. Liq. Cryst., 1977, Vol. 42, pp. 81–96

Printed in Holland

The Stable Inhomogeneities of Mixtures and the Permanent Liquid–Crystalline Diffraction Gratings

ANTONI ADAMCZYK

Institute of Physics, Warsaw Technical University, Koszykowa 75,00-662 Warsaw, Poland

(*Received October 14, 1976; in final form January 19, 1977*)

The stable structural inhomogeneities in nematics/optical active substance solutions have been experimentally investigated. The MBBA or MBBA/EBBA eutectic and abietic acid (AA) as convenient system was chosen. In the solutions of concentrations above some threshold value the creation of separated cholesteric filament regions immersed in nematics were observed, i.e. the distribution of the AA is not homogeneous in nematic liquid. Attempts have been made to interpret the filament structure in terms of the lowest energy configuration of the mixtures.

The regular-band systems of the filament and the lamellar structures play the role of permanent liquid–crystalline diffraction gratings of phase type. The grating constants lie in the range from 0.3 to 3 microns and more. The diffraction is of the Bragg type below the boundary value of the diffraction grating constant and is of the Raman–Nath type above this value. The boundary value was estimated.

1 INTRODUCTION

The appearance of the cholesteric phase in dilute solutions of optical active substances (OAS) in nematic or compensed cholesteric solvents is well known effect. The length of cholesteric pitch P in these solutions is inversely proportional to solute concentration c and is given by equation

$$2\beta Pc = 1 \tag{1}$$

where the coefficient β is the microscopic twisting power of the solute.[1]

In the present work, the investigations of the mechanisms of cholesteric phase creation in nematics/OAS mixtures were performed. The observations were extended to include the effects of light diffraction in lamellar band systems of the cholesterics obtained.

The observations and measurements were made at room temperature on liquid-crystalline solutions of negative dielectric anisotropy with MBBA or MBBA/EBBA eutectic as the nematics, and with abietic acid (AA) as the solute.[2]

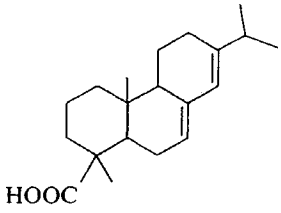

The AA was chosen as the OAS because of its physical properties, mainly of its convenient microscopic twisting power β and surface properties. Its action results in appearance of a clear and undisturbed cholesterics structures in solutions. The cholesterics obtained by means of the AA have sharply visible and stable myelinic and lamellar structures.

Similar investigations were performed with use of other solutions, e.g. with biphenyls as nematics, and with carotenes as solutes, but the results were not so good.

The MBBA and EBBA and biphenyls were synthesized and purified by W. Cwikiewicz and K. Switlak in Institute of Physics of Warsaw Technical University. The AA was a commercial product from Chemapol, Czechoslovakia.

2 DIFFUSION OF OAS INTO HOMEOTROPICALLY ORIENTED NEMATICS LAYERS

In the course of investigations of the cholesteric phase creation, the front of diffusion of the OAS into homeotropically oriented nematics layers was observed with use of polarizing microscope (crossed polarizers). Diffusion was performed in liquid-crystalline layers of geometry as shown in Figure 1. The nematics layer with thickness of about 50 microns was placed between a slide and two cover glasses lying side by side. The nematics was oriented homeotropically (the director is constrained to be perpendicular to the glass surfaces) by coating the glass surfaces with lecithin. The gap between the edges of the cover glasses was filled with some amount of cholesteric 5% AA solution in the same nematics as those placed between the glasses. The AA can propagate from the cholesterics region into the nematic layer, and from diffusion resulting the nematics layer has a slightly graded concentration profile with a very low AA concentration near the front of diffusion. The

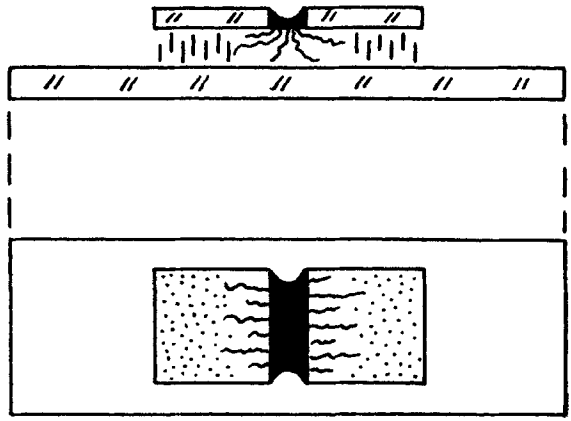

FIGURE 1 Geometry of liquid-crystalline layer used in observation of front of diffusion of the OAS into homeotropically oriented nematics.

nematic regions distant from the front exhibits behavior characteristic for a pure homeotropic texture. The part of the liquid-crystalline layer disturbed by action of the solute was sharply visible on the dark background of homeotropic texture between crossed polarizers.

The front of expansion of cholesteric phase into the volume of the nematic layer is initially visible as a series of separated fringes (Figure 2). Every fringe consists of an axial cholesteric core surrounded with a bright cover of deformed nematics. The length of the fringes increases versus time although some dissolution of the cholesteric core is visible on its top.

A later stage of diffusion the series of isolated myelinic filaments appears, and the relative thickness of the cover of deformed nematics decreases in this stage, Figure 3. Completely isolated myelinic filaments are shown in Figure 4. It is visible that the bend deformation of the filaments results in twist deformation of these filaments. This twist deformation is distinctly visible in the case of toroidal forms of myelinic filaments as shown in Figure 5. A deformation of the myelinic filament as a result of contact between the filament and the glass surfaces is also visible in this picture. The part of the myelinic filament anchored on the glass surfaces is probably transformed into a lamella. Figure 6 shows the crossing of three myelinic filaments and, moreover, two other myelins oriented perpendicular to the glass surfaces. Similar perpendicularly oriented or skewed myelins are represented in Figure 7. The perpendicularly oriented myelins are to a certain extent regularly ordered in large ensembles, Figure 8. The conformation presented in Figure 8 is very stable and was observed over many days.

The polarizing microscope pictures of thick myelins, anchored perpendicularly on the glass surfaces, show their internal structure. The myelinic

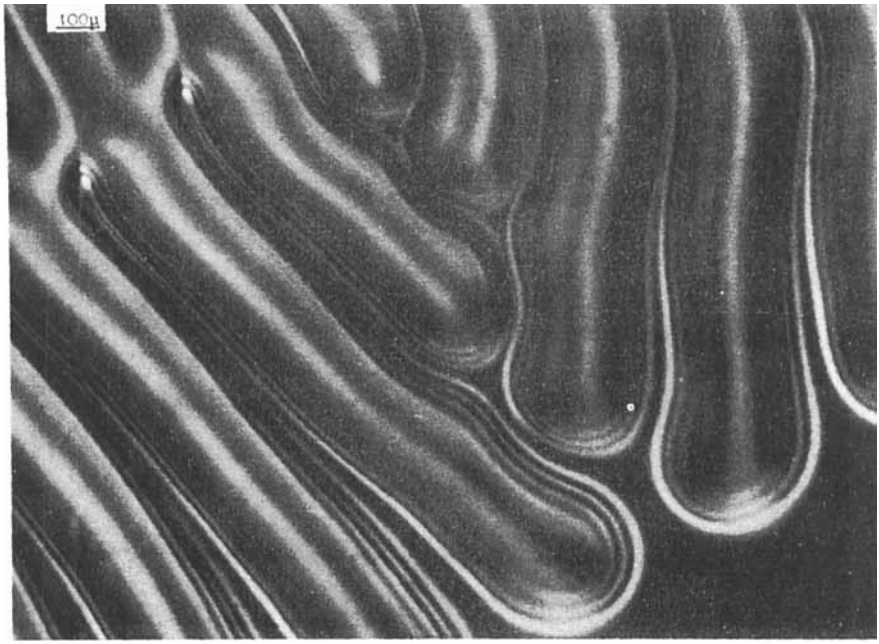

FIGURE 2 The initial stage of front of diffusion of the AA into the MBBA layer.

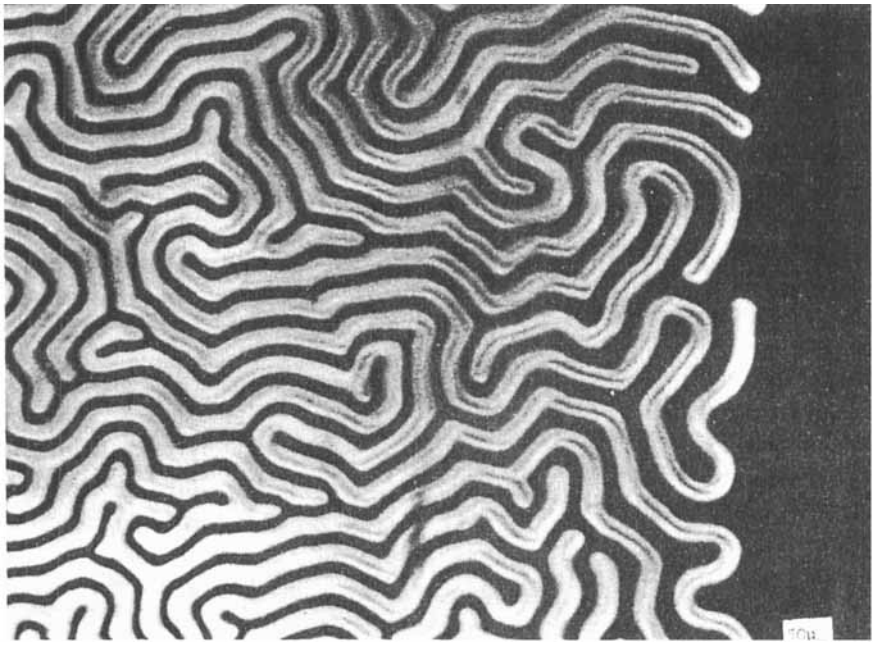

FIGURE 3 Later stage of front of diffusion.

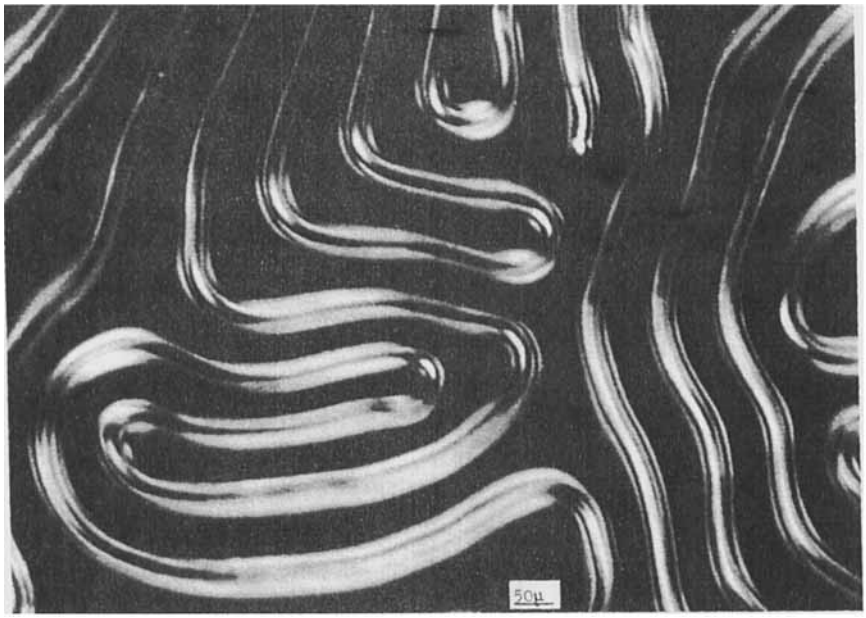

FIGURE 4 Completely separated myelinic filaments of cholesteric type immersed in homeotropically oriented nematics.

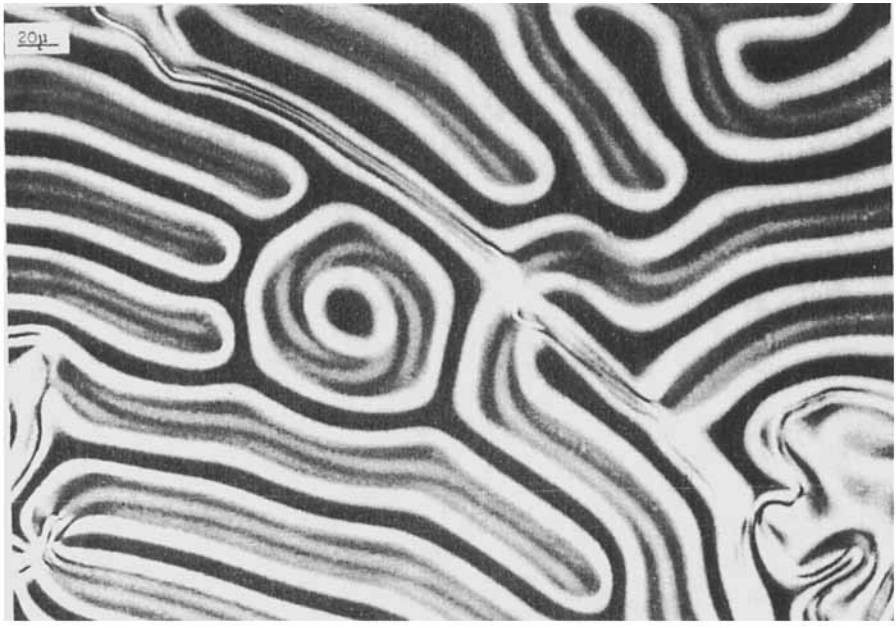

FIGURE 5 The toroidal myelinic filament. The twist deformation is acted by bend.

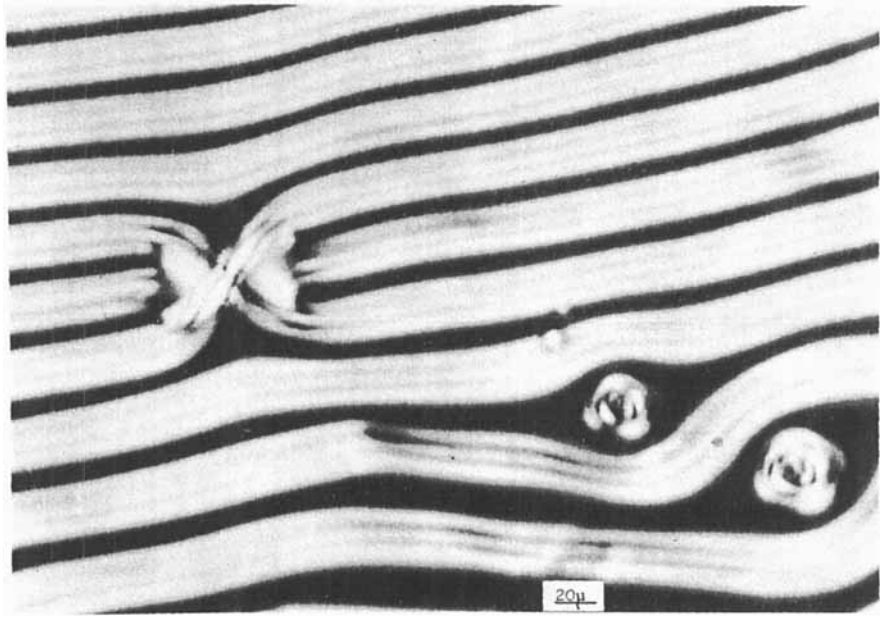

FIGURE 6 The crossing of three filaments. Two perpendicularly oriented filaments are also visible.

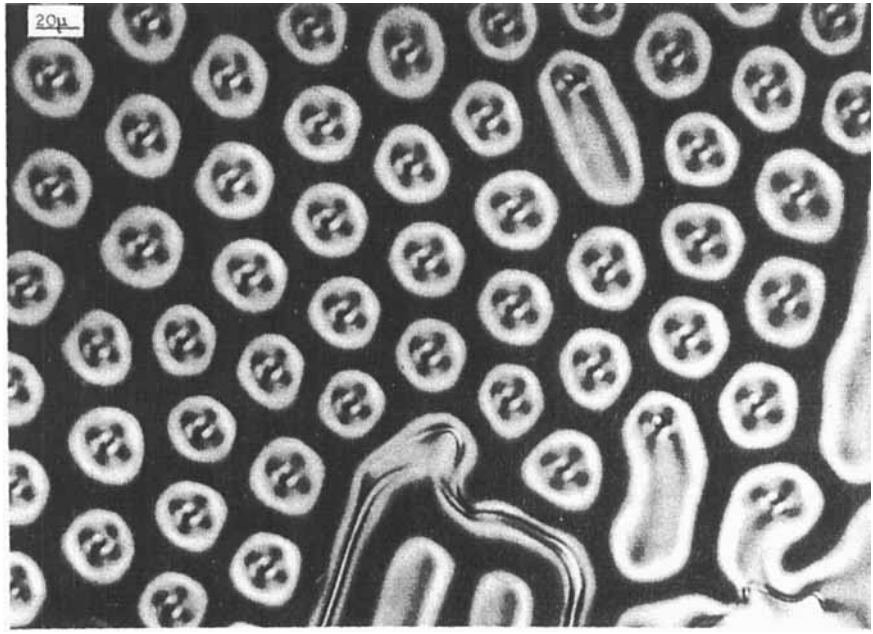

FIGURE 7 Perpendicularly oriented and skew myelins immersed in nematics.

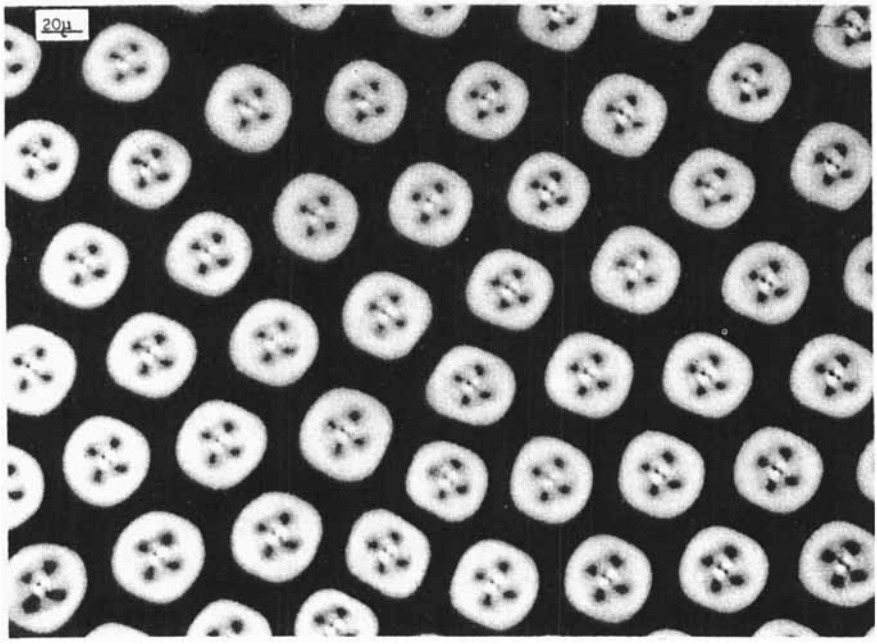

FIGURE 8 Symmetrically ordered big ensemble of perpendicularly oriented myelins immersed in nematics.

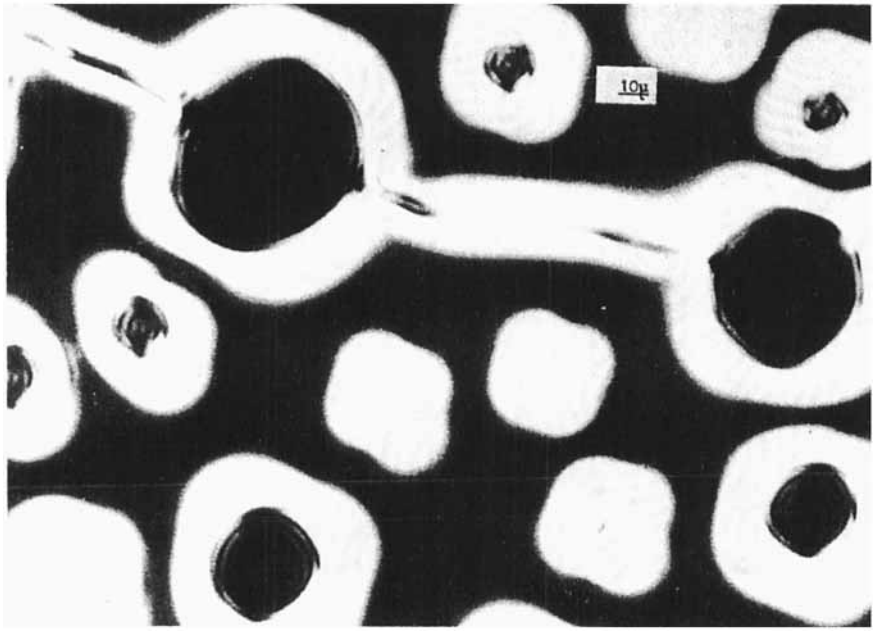

FIGURE 9 The coaxial layered internal structure of cholesteric cores of myelins.

FIGURE 10 The myelinic–lamellar structure observed in a "thick" layers.

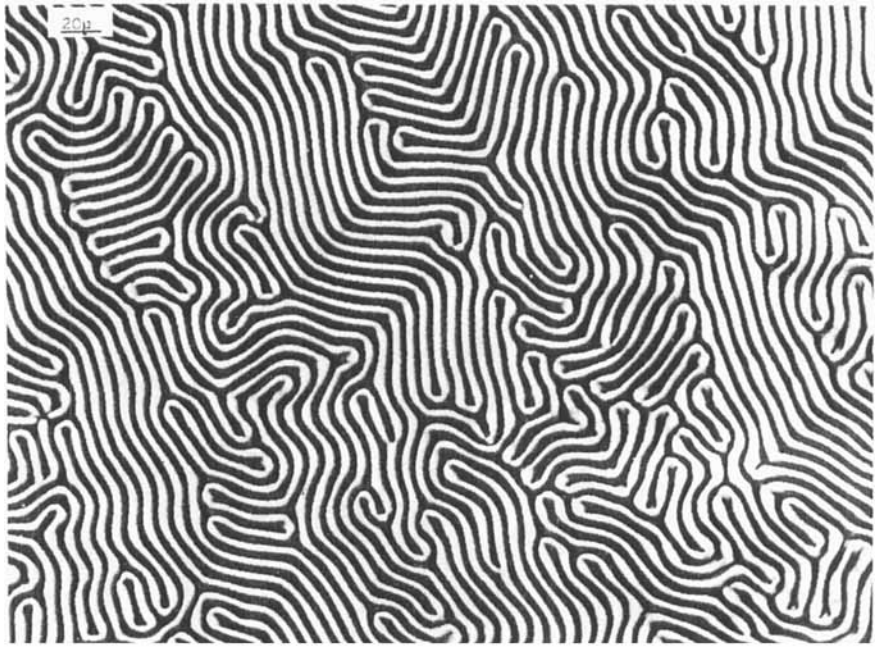

FIGURE 11 The dense packed lamellar labyrinth.

filaments presented in Figure 9 have a coaxial layered structure, and very thick myelins are mutually connected with lamellar walls. In thick samples, the mixed myelinic and lamellar structures form topologically complicated figures similar to some biological objects, Figure 10. In thin samples, thickness of which is comparable with the diameters of the myelins, the myelinic–lamellar structures form dense-packed, beautiful, linear patterns, Figure 11.

3 THE STABLE INHOMOGENEITIES IN MIXTURES OF NEMATICS AND OPTICAL ACTIVE SUBSTANCES

The fact that the OAS added to nematics gives separated, and immersed in nematic phase, cholesteric myelins may be interpreted as a result of a process of equilibration in which the solute distributes inhomogeneously inside the solution, and local cholesterics regions appear in the spaces with higher concentrations of the solute. Creation of separated cholesterics regions is possible only when the free energy F of the solution decreases as a result of phase transition from nematic to cholesteric phase in some part V_c of total volume of solution V_0.

The cholesterics myelins, immersed in nematics, are stable in solutions in which concentrations $c = n_D/n_N$ (where n_D and n_N are the total numbers of molecules of the OAS and the nematics, respectively) exceed some threshold value c_t. Thus the free energy F must be decreased in the presence of the cholesterics regions. Simple calculation confirms this suposition. When P, V, and T are constant, then for chemical potentials and for energy of the cholesteric spontaneous torsion the inequality below must be satisfied

$$\Delta F_{NN} + \Delta F_{DN} > \Delta F'_{NN} + \Delta F'_{DN} + \Delta F'_{NC} + \Delta F'_{DC} + \int_0^{V_c} g_{\text{def}}\, dV \qquad (2)$$

where g_{def} is density of free energy of the cholesteric torsion, and ΔF_{ik} are the "chemical" parts of free energy: $\Delta F_{NN} = \mu_N n_N$, $\Delta F_{DN} = \mu_D n_D$, $\Delta F'_{NN} = \mu_N(n_N - n_{NC})$, $\Delta F'_{DN} = \mu_D(n_D - n_{DC})$, $\Delta F'_{NC} = \mu'_N n_{NC}$, $\Delta F'_{DC} = u'_D n_{DC}$. The μ_N and μ'_N are the chemical potentials of the nematogen, and μ_D and μ'_D are the chemical potentials of the OAS in nematic and cholesteric phases, respectively. Numbers of molecules of the nematogene and of OAS in the cholesteric phase are denoted by n_{NC} and n_{DC}, respectively.

Substitution of ΔF_{ik} from above to (2) gives

$$\mu_N n_N + \mu_D n_D > \mu_N(n_N - n_{NC}) + \mu_D(n_D - n_{DC}) + \mu'_N n_{NC} + \mu'_D n_{DC} + \int_0^{V_c} g_{\text{def}}\, dV \qquad (3)$$

or in reduced form

$$\mu_N n_{NC} + \mu_D n_{DC} > \mu'_N n_{NC} + \mu'_D n_{DC} + \int_0^{V_c} g_{\text{def}}\, \mathrm{d}V \tag{3'}$$

In state of thermodynamic equilibrium the chemical potentials must fulfil the equations

$$\begin{aligned} \mu_N &= \mu'_N \\ \mu_D &= \mu'_D \end{aligned} \tag{4}$$

Taking into consideration the equation (4), as the condition of co-existence of nematic and cholesteric phases we find

$$\int_0^{V_c} g_{\text{def}}\, \mathrm{d}V < 0 \tag{5}$$

This condition is fulfilled always because the spontaneous cholesteric torsion gives a negative contribution to the total free energy of the system.

The above consideration is based on the assumption that the free energy associated with cholesteric torsion is much larger than this associated with the creation of the interface. This means that the sum

$$\int_S g_s\, \mathrm{d}S + \int_0^{V_c} g_{\text{def}}\, \mathrm{d}V < 0 \tag{6}$$

where S is the total surface of the interface, and g_s is density of the surface free energy.

The threshold concentration c_t of the OAS may be estimated on the ground of the equations (4) and in assumption that the chemical potentials of the nematogene and the OAS are expressed as:[3]

$$\begin{aligned} \mu_N &= \mu_0 - kT\frac{n_D}{n_N}, \\ \mu'_N &= \mu'_0 - kT\frac{n_{DC}}{n_{NC}}, \\ \mu_D &= kT \ln \frac{n_D}{n_N} + \Psi, \\ \mu'_D &= kT \ln \frac{n_{DC}}{n_{NC}} + \Psi', \end{aligned} \tag{7}$$

where $\mu_0 = \mu_0(P, T)$ and $\mu'_0 = \mu'_0(P, T)$ are the chemical potentials of the nematogene in the nematic and the cholesteric phases, respectively, and $\Psi = \Psi(P, T)$ and $\Psi' = \Psi'(P, T)$ are the characteristic potentials of the solution in the nematic and the cholesteric phases, respectively.

If the concentration n_D/n_N is equal to the threshold value c_t then the concentration in the cholesterics region n_{DC}/n_{NC} may be expressed in form $c_t + \delta$ where δ is small compared with c_t. Substitution of adequate expressions from (7) to equations (4), and use of the approximation that $\ln(c_t + \delta) = \ln c_t + \delta/c_t$ gives the equations

$$\begin{aligned} kT\delta &= c_t(\Psi - \Psi') \\ kT\delta &= \mu_0' - \mu_0 \end{aligned} \tag{8}$$

and the threshold concentration c_t takes the form

$$c_t = \frac{\mu_0' - \mu_0}{\Psi - \Psi'} \tag{9}$$

The equation (9) is the evidence that the threshold concentration c_t has a low value in two cases: (i) when the nematics easily "goes into" the cholesteric phase, (ii) when the difference between thermodynamic properties of the solution in the nematic and in the cholesteric phases is large. It is clear that the equation (1) is not applicable at all concentration values.

4 THE RAMAN–NATH DIFFRACTION AND THE BRAGG DIFFRACTION IN THE PERMANENT LIQUID–CRYSTALLINE DIFFRACTION GRATINGS

The direction of the cholesteric axis with respect to glass surfaces is usually determined by the boundary conditions, and some techniques have been devised for the preparation of oriented cholesteric films. In particular, the cholesteric axes of the myelinic and lamellar structures may be oriented parallel with respect to glass surfaces (fingerprint pattern). It is possible only when the thickness of the cholesterics film is compared with the widths of lamellae. In thick cholesterics layers this orientation is impossible because of natural tendency of cholesterics to adopt the focal-conic texture formation as in the case of droplets shown in Figure 12. In band systems of oriented myelinic filaments and lamellae the optical properties change almost sinusoidally in direction perpendicular to the cholesteric axis. A periodic change of molecular orientation difference corresponding to the alternation of dark and bright bands, Figure 13, gives rise to the possibility of application of these band systems as a permanent diffraction gratings. The permanent cholesteric diffraction gratings differ from those obtained with use of periodic electrohydrodynamic instabilities in nematics.[4,5] The main difference is that the diffraction grating constants are of the value from 0.3 to about 3 microns in the case of permanent diffraction gratings, whereas in electrohydrodynamic diffraction gratings these constants are about of 5 microns and more.

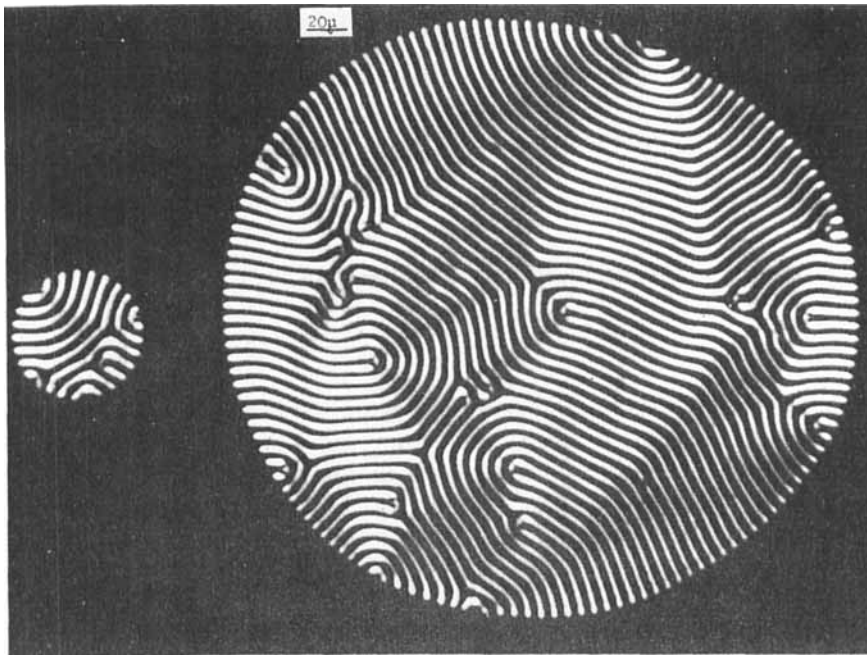

FIGURE 12 The focal-conic texture in the droplets of 5% solution of MBBA/AA.

Diffraction of light on the cholesteric diffraction gratings is to some extent similar to that observed on diffraction gratings excited by ultrasonic waves in transparent solid or liquid layers. The theory of these diffraction gratings predicts two types of diffraction:[6,7] the Raman–Nath diffraction in the case when $q^2L/k < \pi$, and the Bragg diffraction when $q^2L/k > \pi$, where q is wave vector of periodic deformation in diffraction grating, and k is wave vector of light, and L is length of path of light wave in diffraction grating (for small angles of incidence it is equal to thickness of the diffraction grating).

In the case of the Raman–Nath diffraction, i.e. for a "thin" cholesteric diffraction gratings, the angle positions of the main diffraction maxima are given by equation

$$\sin \theta_m = m \frac{\lambda}{P} \tag{10}$$

where m is the order of the maximum, and P is the cholesteric pitch, and λ is wavelength of light. Neglecting the complicated dependence between optical anisotropy of liquid-crystalline film and a state of polarization of

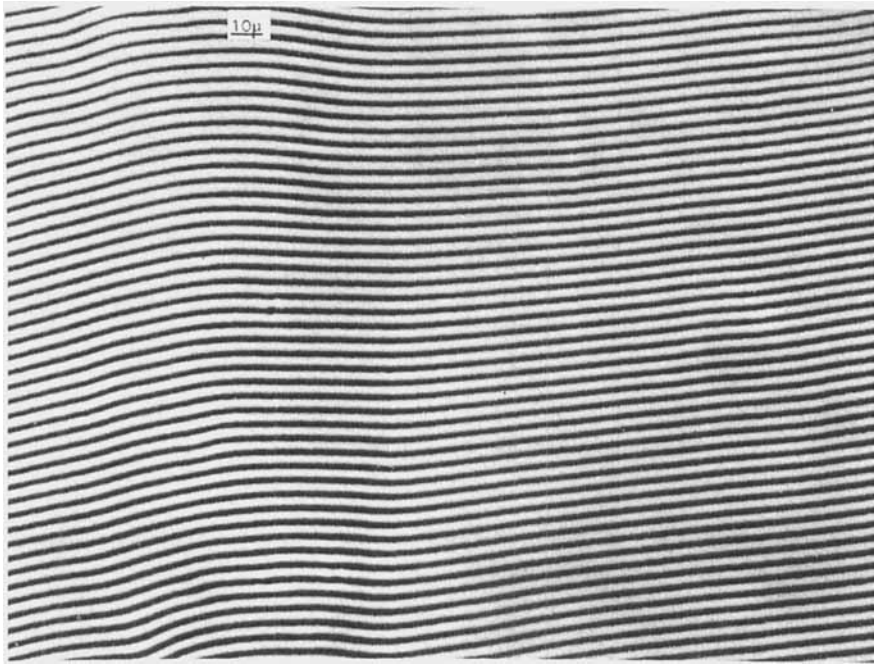

FIGURE 13 The oriented and partially ordered fingerprint pattern. The band system acts as a sinusoidal diffraction grating of the phase type.

incident light, for the light intensity in the main maxima, we have

$$I_m = I_0 J_m^2\left(\frac{2\pi}{\lambda} L\Delta n\right), \tag{11}$$

where I_0 is the incident light intensity, and J_m is the m-order Bessel function, and Δn is the amplitude of change of the refractive index of liquid-crystalline layer.

The Bragg diffraction occurs for "thick" diffraction gratings, i.e. when the light beam is passed across many wave fronts of diffraction grating.[8] In the case of Bragg diffraction on sinusoidal diffraction gratings of the phase type the non-zero intensity maxima are of 0 and ± 1 orders only.

For the angle of incidence θ_0 the first-order Bragg diffraction angle is $-\theta$, Figure 14, and relationship between them may be written as

$$\sin\theta = \sin\theta_0 + \frac{q}{k} = \sin\theta_0 + \frac{\lambda}{P} \tag{12}$$

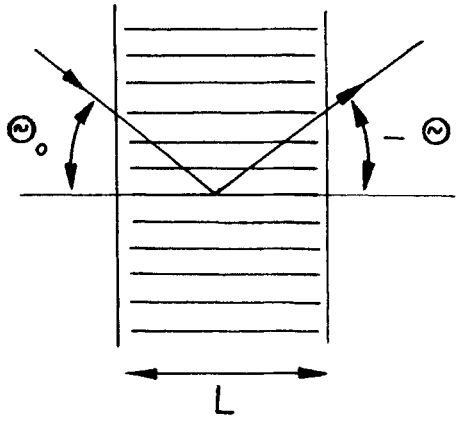

FIGURE 14 Diagrammatic sketch of the Bragg diffraction.

The light intensity in the first-order maximum is the biggest one for incidence angle θ_0 satisfying the condition:

$$\sin \theta_0 = -\frac{\lambda}{2P} \tag{13}$$

i.e. when $\theta = -\theta_0$. This angle θ_0 is called the Bragg angle. When incidence angle is equal to the Bragg angle the light intensity in the first-order maximum is given by equation

$$I_1 = I_0 \sin^2 \frac{\pi L}{\lambda} \Delta n \tag{14}$$

Estimation of the type of diffraction, performed following the criterion

$$\frac{q^2 L}{k} = \pi \tag{15}$$

for $L = 25$ microns, and for He–Ne laser light ($\lambda = 633$ nm), gives the boundary value of cholesteric pitch $P = 7$ microns as a result. Then for $P > 7$ microns there is the Raman–Nath diffraction, and for $P < 7$ microns the Bragg diffraction occurs in conditions as above.

The Raman–Nath diffraction occurs only at very small incidence angles and, as a rule, gives a series of maxima.

Practically, the permanent liquid-crystalline diffraction gratings are of the Bragg type and the first-order maximum appears only. Very weak second-order maximum, as observed in some cases, is probably resulting from deformation of the band structure. The Bragg angles for the permanent

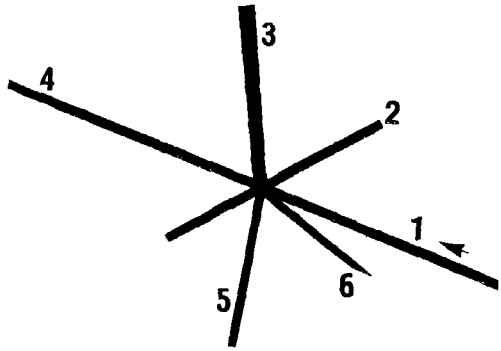

FIGURE 15 The photograph of He–Ne laser beam incident on the permanent liquid-crystalline diffraction grating. The photograph was made in a dark and smoky room. 1-incident beam, 2-diffraction grating, 3-diffracted beam, 4-transmitted beam (zero-order), 5-reflected beam, 6-weak back-diffracted beam.

diffraction gratings are usually very large (often larger than 45°). It means that the cholesteric pitch P is comparable with wavelength of light. Figure 15 shows the photograph of He–Ne laser beam incident on the permanent liquid-crystalline diffraction grating. The photograph was made in a dark and smoky room. The incidence angle of the laser beam 1 is a little larger than the Bragg angle to show the weak back-diffracted beam 6 which is symmetrical to the ordinary diffracted beam 3.

The permanent liquid-crystalline diffraction gratings have large resolving power and give partially polarized diffracted light of large intensity. Due to very small grating constants and the phase character of these gratings the diffraction rainbow is clear and very bright with the angular width of about 45° from 50° to 95° for wavelengths 422 and 741 nanometers, respectively. Contained to avoid evaporation of chemical agents these gratings are stable over several months at room temperature.

After convenient treatment of glass surfaces the permanent liquid-crystalline diffraction gratings of size of 90 × 120 mm with the density of the bands of about 2,500 mm^{-1} and with a good homogeneity can be easily obtained.[9]

5 CONCLUSIONS

Dilute solutions of nematic liquid crystals as solvents, and of optical active substances as solutes, were investigated. In some range of concentration of the solute, the stable structural inhomogeneities were found to appear in investigated solutions, especially in solutions of the abietic acid as the solute

and of the MBBA or MBBA/EBBA eutectic as the solvents. The threshold concentration of the solute c_t, above which the inhomogeneities appear, depends on thermodynamic characteristics of the solute and of the solvent in both nematic and cholesteric phases (equation (9)). For solute concentrations $c \leq c_t$ the solution has the nematic phase only. In the solutions of concentrations of range from c_t up to $c_t + \delta$, where δ may be estimated as $\delta = \mu'_0 - \mu_0/kT$, the co-existence of both the nematic and the cholesteric phases appear. At lower concentrations inside this range only the separated myelinic filaments of cholesteric structure appear, and at higher concentrations the filaments are partially connected together resulting in appearance of mixed myelinic–lamellar systems. When the concentrations are $c \geq c_t + \delta$, then the solutions are solely of the cholesteric phase with lamellar structure type, and the cholesteric pitch P is approximately given by equation (1).

The process of transformation of myelinic filaments to the myelinic–lamellar structures depends not only on solute concentration but also on the thickness of the layer of liquid crystal, and on boundary conditions.

Cholesteric myelinic and myelinic–lamellar structures, as observed with the use of polarizing microscope, are quite similar to certain electron-microscope pictures of biological structures.

Cholesteric lamellar structures may be oriented to give a fingerprint pattern. The band systems in this pattern may be partially ordered in one direction. These ordered band systems play a role of permanent liquid–crystalline diffraction gratings of the phase type giving light diffraction of the Bragg type. The most suitable cholesterics for the purpose are those with pitch P in the range from 0.3 to 3 microns.

There are still some open questions the elaboration of effective methods of the glass surface treatment to form the stable, oriented, and ordered band systems.

References

1. P. G. de Gennes, The Physics of Liquid Crystals, Clarendon Press, Oxford, 1974.
2. A. Adamczyk, Polish Patent Announcement No. 179159, March 28th 1975.
3. L. D. Landau, and E. M. Lifschitz, Statistical Physics, Pergamon, London, 1958.
4. L. K. Vistin, *Soviet Phys. Cryst.*, **15**, 514 (1970).
5. W. Greubel and U. Wolff, *Appl. Phys. Lett.*, **19**, 213 (1971).
6. M. Born and E. Wolf, Principles of Optics, Pergamon, Oxford, 1968.
7. J. W. Tucker and V. W. Rampton, Microwave Ultrasonics in Solid State Physics, North-Holland, Amsterdam, 1972.
8. G. W. Willard, *J. Acoust. Soc. Amer.*, **21**, 101 (1949).
9. A. Adamczyk, Permanent liquid-crystalline diffraction grating (The model). Polish–Russian Chemical Exhibition, Wroclaw, May 7–14th, 1975.